Simple *in Situ* Monitoring of a Complex Catalytic Reaction Network at High Pressure by Attenuated Total Reflection Fourier Transform Infrared Spectroscopy

JEAN-MICHEL ANDANSON, FABIAN JUTZ and ALFONS BAIKER*

Institute for Chemical and Bioengineering, Department of Chemistry and Applied Biosciences, ETH Zurich, Hönggerberg, HCI, CH-8093 Zürich, Switzerland

Attenuated total reflection (ATR) Fourier transform infrared (FT-IR) *in situ* measurements were performed during the catalytic hydrogenation of acetophenone under high pressure (5.0 MPa). The catalyst used was a suspension of rhodium nanoparticles in an ionic liquid. At the highest temperature used (80 °C), the selectivity of the hydrogenation to 1-phenylethanol dropped from 80% in the beginning of the reaction, when acetylcyclohexane was the main side product, to less than 50% after a few hours of experiment because of the consecutive hydrogenation of 1-phenylethanol to ethylcyclohexane. The evolution of the concentrations of reactant and products was quantified using flawless spectra of pure components with a classical least squares (CLS) multivariate method applied to several ranges of the mid-infrared spectra. The only variable parameters of the analysis are the concentrations of each component themselves and the baseline shift of the spectrum during the reaction. The advantage of using multivariate analysis over the analysis of a single vibrational band, as well as the limitations of this type of spectral analysis, are discussed.

Index Headings: **In situ; Attenuated total reflection; ATR; Fourier transform infrared spectroscopy; FT-IR spectroscopy; Hydrogenation; Kinetics; Catalysis; Spectra deconvolution; Multivariate analysis.**

INTRODUCTION

Monitoring catalytic reactions using *in situ* infrared spectroscopy has gained growing attention in the past decade.[1–7] In a batch reactor, the reaction time is a crucial parameter when the goal is to achieve good selectivity to the desired product in a complex reaction network consisting of parallel and/or consecutive reactions. The best way to gain complete information about the kinetics is to follow *in situ* the concentration changes of each reactant and product during the process, using a nondestructive technique. Consumption of hydrogen,[8] chromatography,[9,10] and spectroscopy[3,11–13] are some of the techniques generally employed to measure the progress of hydrogenation reactions. One of the main advantages of spectroscopy is its ability to detect and quantify several components and possible interactions, even under high pressure, without the need to take samples from the reaction system. The challenge is then to efficiently analyze the overall dataset in order to extract the concentration of each single component of the system at several points in time during the reaction. In the case of a non-ideal chemo-selective hydrogenation, a strong overlapping of the bands between species makes it difficult to quantify the reaction products by a simple univariate analysis (e.g., the intensity of one single wavenumber of the spectrum or the intensity of one specific band corresponding to one specific vibration). Numerous multivariate methods have been developed in recent years to analyze infrared spectra of complex samples. In the present investigation we have chosen the rhodium-catalyzed hydrogenation of acetophenone (AP) to study *in situ* chemo-selective hydrogenation using attenuated total reflection (ATR) Fourier transform infrared (FT-IR) spectroscopy.

The hydrogenation of aromatic ketones has been extensively studied over the past years because of its major importance in chemistry. AP hydrogenation has been performed with various catalysts in liquid phase[10,13–17] and in gas phase.[18] Selective hydrogenation of the carbonyl group yielding 1-phenylethanol (PE) is particularly interesting as PE is useful in the fragrance industry[19] or as an intermediate. The hydrogenation of the aromatic ring producing acetylcyclohexane (AC) and hydrogenolysis of the alcohol group both generate unwanted side products. The possible reactions from AP with hydrogen are summarized in Scheme 1.

One of the most challenging aspects of organic chemistry is the necessity to achieve an easy separation between products and solvents after reaction. In recent years the use of ionic liquids (IL) as media for catalytic reactions has emerged as a promising new method[20] since ILs normally have negligible vapor pressures.[21,22] The extraction of products from IL/nanoparticles can be done easily and recycling of the nanoparticles is simple. Plenty of current studies are using catalytically active nanoparticles in ILs, as nanoparticles are stabilized by ILs and can be synthesized directly inside ILs.[23–26] Scheeren et al. showed by means of X-ray photoelectron spectroscopy (XPS) that ILs are able to form a protective layer surrounding the platinum nanoparticles.[23] The hydrogenation reaction focused upon in the present study is catalyzed by rhodium nanoparticles suspended in one of the most frequently used ILs (1-butyl-3-methylimidazolium hexafluorophosphate; [bmim][PF_6]) directly mixed with AP without the use of any solvent. ATR spectroscopy is used to measure *in situ* the evolution of the reactant and products at room temperature (RT) and 80 °C under 5.0 MPa of hydrogen

In situ ATR spectroscopy has been employed to analyze chemical interactions and quantify molecular species in solid and liquid materials within catalysis,[14] polymers,[27] or supercritical fluids[28] applications. In the past decades, various chemometrics methodologies have been developed to examine experimental data (in analytical chemistry), and some methods have been developed for ultraviolet (UV), near-IR (NIR), or mid-IR spectroscopy. An introduction and some details on multivariate analysis can be found in reviews, e.g., Refs. 29 and 30. A plethora of models have been developed over the years for many kinds of systems: food chemistry, the pharmaceutical industry, and the polymer industry, as well as for biological and other applications. Basically, models can be

Received 17 July 2009; accepted 14 December 2009.
* Author to whom correspondence should be sent. E-mail: baiker@chem.ethz.ch.

0003-7028/10/6403-0286$2.00/0

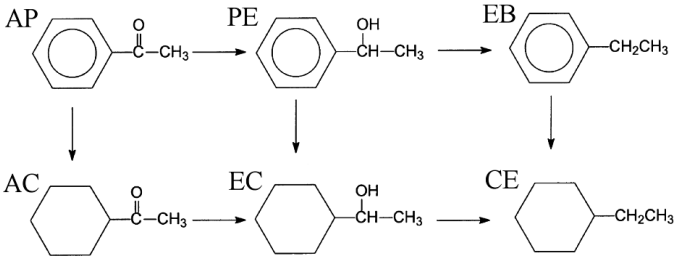

SCHEME 1. Possible reactions from AP with hydrogen.

classified according to cases where all compounds are well known and the spectrum of each compound can be used as an input for the model, and cases where this information is not available. In our case, in which the IR spectrum of each component is known and even having the opportunity to perform calibrations using several known solutions of the system, the multivariate analysis chosen is a straightforward multiple linear regression (MLR). In mid-IR spectroscopy, Chan et al. combined *in situ* ATR with FT-IR imaging and a simple multivariate analysis (classical least squares, CLS) in a pharmaceutical application estimating the amount of paracetamol in hydroxypropylmethylcellulose (HPMC).[31] Recently, Kriesten et al. presented results of a refined method (indirect hard modeling, IHM) taking care about modification of the spectra due to molecular interactions.[32] Here we elucidate the practical potential of an extremely simple multivariate analysis on mid-IR spectra using the rhodium-catalyzed hydrogenation of AP under high pressure as an example.

EXPERIMENTAL DETAILS

1-butyl-3-methylimidazolium hexafluorophosphate [bmim][PF_6] (99% purity, product no: AB172327), 1-cyclohexanol (CE) (98%), 1-phenylethanol (PE) (98%), and $Rh(OAc)_3$ (99.9%) were purchased from ABCR, acetophenone (AP) (99%) was obtained from Acros Organics, ethylcyclohexane (EC) (>99%) and ethylbenzene (EB) (99.8% purity) were obtained from Aldrich, acetylcyclohexane (AC) was obtained from Alfa Aesar (purity 95%), and dense CO_2 was supplied by Pangas (99.995% purity) and used without any further purification.

The nanoparticles were prepared by mixing 0.216 g (0.77 mmol) of $Rh(OAc)_3$ with 1.34 g (4.72 mmol) of [bmim][PF_6] and transferring the mixture into a 100 mL stainless steel autoclave. The reactor was flushed three times with H_2 and then pressurized with 3.0 MPa H_2. The mixture was heated to 60 °C and stirred overnight. To remove the precursor ligand, the mixture was extracted with supercritical CO_2 at 9 to 10 MPa and 50 °C over 5 h. Finally, 1.4 g of a black viscous mixture was obtained, which was then used as a catalyst (8% w/w of Rh in IL) without further treatment.

A high pressure cell with variable volume and several optical probing paths was used for the spectroscopic experiments. **Safety note:** *High pressure experiments require special equipment with the appropriate pressure rating.* The cell is equipped with two sapphire windows to allow direct observation of the phase behavior. In addition, it is equipped with two ZnSe windows for transmission infrared measurements in the gas phase and a ZnSe internal reflection element on the bottom to study the liquid phase. The details of the cell used in the work are described elsewhere.[14] Spectra were measured with an IFS-66 spectrometer (Bruker Optics) with a resolution of 2 cm^{-1} in the range of 4000–600 cm^{-1}. During the hydrogenation reaction a spectrum was taken every 10 minutes using a mercury cadmium telluride (MCT) detector. The surface-enhanced infrared absorption (SEIRA) due to the presence of metallic nanoparticles[33] was not observed in our measurements; therefore, this effect has not been considered in the following analysis. Moreover, the variation of the refractive index of the solution during the experiment has been considered as negligible as the refractive index of the product and reactant are very similar. Each experiment was started by first flushing then adding H_2 to the system (8 mg of nanoparticles suspended in 92 mg ionic liquid, with 1 g of acetophenone) up to a pressure of 5.0 MPa. Finally, all analysis and fitting procedures were performed with a least squares method employing Gnuplot 4.2 software and using authentic spectra of the solution without any prior baseline, spectral subtraction, or smoothing treatment. The reproducibility of the overall method under various reaction conditions has been shown in Ref. 34 (Fig. 7).

After opening the reactor, the reaction mixture was analyzed by a gas chromatograph (GC) (Thermoquest Trace GC, CE Instruments) equipped with an HP-FFAP capillary column (30 m × 0.32 mm × 0.25 μm) and a flame ionization detector (FID).

DETAILS OF THE MODEL

A pure spectrum of each component of the mixture was measured and deconvoluted in a sum of Gaussian functions. Infrared spectra of pure reactant and products and the model spectrum are presented in Figs. 1 and 2. Using this approach, each spectrum is described as a function:

$$F_i(\nu) = \Sigma_j G_j(\nu) \quad (1)$$

where $F_i(\nu)$ is the model of an experimental spectrum of a pure compound and $G_j(\nu)$ corresponds to a single Gaussian function. Then, the description of a solution is simply given by a summation of the individual spectra weighted by their relative concentrations:

$$S(\nu) = \Sigma_i a_i F_i(\nu) \quad (2)$$

More details and an extensive discussion about the spectral model fit, CLS, and IHM can be found elsewhere.[32] It was chosen not to work directly with the spectra of the pure compounds but with a simple mathematical representation to remove the noise, baseline shift, vapor water signals, or other small occurrences that could perturb the fitting of a spectrum corresponding to a solution ($S(\nu)$). For example, if one of the experimental spectra of a pure compound was "contaminated" by some vapor water when the spectrum of a solution also contains some vapor water, the concentration of that particular element would be wrongly increased without explanation. As the infrared spectra of one molecule can be changed with its environment, it is not necessarily realistic to try to simulate a solution as a sum of individual spectra of pure compounds. Another approach could be to use, for example, the band-target entropy minimization (BTEM) model developed by Garland and co-workers.[35] BTEM is a self-modeling curve resolution (which does not require any spectral libraries) that has been used, for example, to follow the catalytic hydrogenation of ketones.[6,13] The idea of the model is to build several (as few as

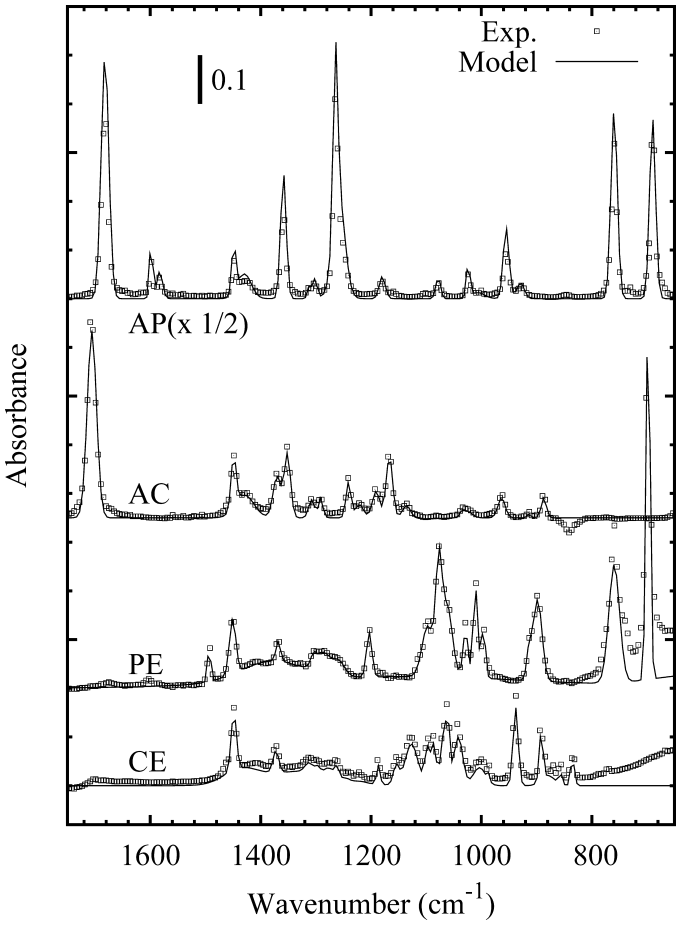

FIG. 1. ATR FT-IR spectra of pure AP, AC, PE, and CE and the model spectrum in the fingerprint range.

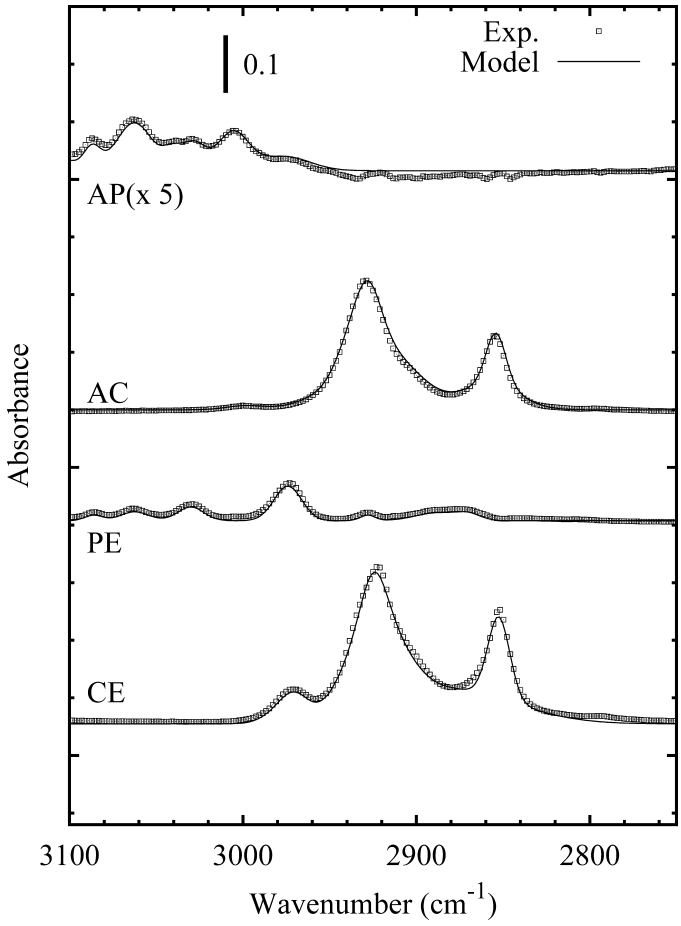

FIG. 2. ATR FT-IR spectra of pure AP, AC, PE, and CE and the model spectrum in the CH stretching range.

possible) spectra that are together able to reconstruct any spectra of the initial dataset. Then, each spectrum is linked to a pure component and finally the concentration of each component can be estimated for any experimental spectrum.

As in our case it is possible to exploit the spectrum of each single component, we choose the other method, using the simple decomposition of the experimental spectrum by the sum of the model spectra of the individual components. Nevertheless, in this approach some bands had to be taken very carefully. For example, the position and intensity of the OH stretching vibration can be drastically changed with the structure of the fluid even at constant temperature for a pure fluid. Models to quantify hydroxyl groups and hydrogen bonds in solution are still possible but become extremely complex.[36,37] Other particular bands, present in our studies, including the C=O stretching mode situated around 1700 cm^{-1} (which can shift with the presence of hydroxyl groups, creating hydrogen bonds with the carbonyl group[38,39]) and the PF_6^- vibration of the ionic liquid (which is sensitive to charge distribution[28]), are also known to be perturbed by the local organization around them. Therefore, particular attention should be given to these bands; it is possible to simply bestow some flexibility on the position (or/and intensity, width) of these bands, or even better, improve the model by calculating the position of the band as a function of known parameters such as the concentration of each component in the solution. For example, the position of the C=O stretching bands shift with the concentration of hydroxyl groups created during the hydrogenation, and then, knowing the concentration of each product, it should be possible to change the shift of the position of the Gaussian function corresponding to the C=O band(s) without adding any extra variables. Finally, it is also important to deal with the spectra of pure components very carefully because it is not realistic to try to fit the spectrum of a molecule dissolved in solvent to its spectrum in crystalline form, as even the spectra of crystalline and amorphous forms of a substance are different.[40] Not all effects are easily anticipated; for example, the position of the PF_6^- band in solution with AP is shifted by more than 20 cm^{-1} compared to the same band in the highly concentrated nanoparticle suspension.

In the present case, the hydrogenation of AP, we chose to work with two different models. The first one we call fingerprint (FP), as it largely uses the range of the fingerprint region of the infrared spectra (in the range from 1800 to 650 cm^{-1}), whereas the second model focuses only on the CH stretching band (CH model in the range from 3150 to 2750 cm^{-1}). After initial testing of the procedure by measuring solutions with known concentrations, it appeared necessary to take into account the small variation of the baseline:

$$S(\nu) = \Sigma_i a_i F_i(\nu) + c \qquad (3)$$

where c is a constant. To decrease the problem of the baseline and remove signals from solvents and catalyst from the spectra,

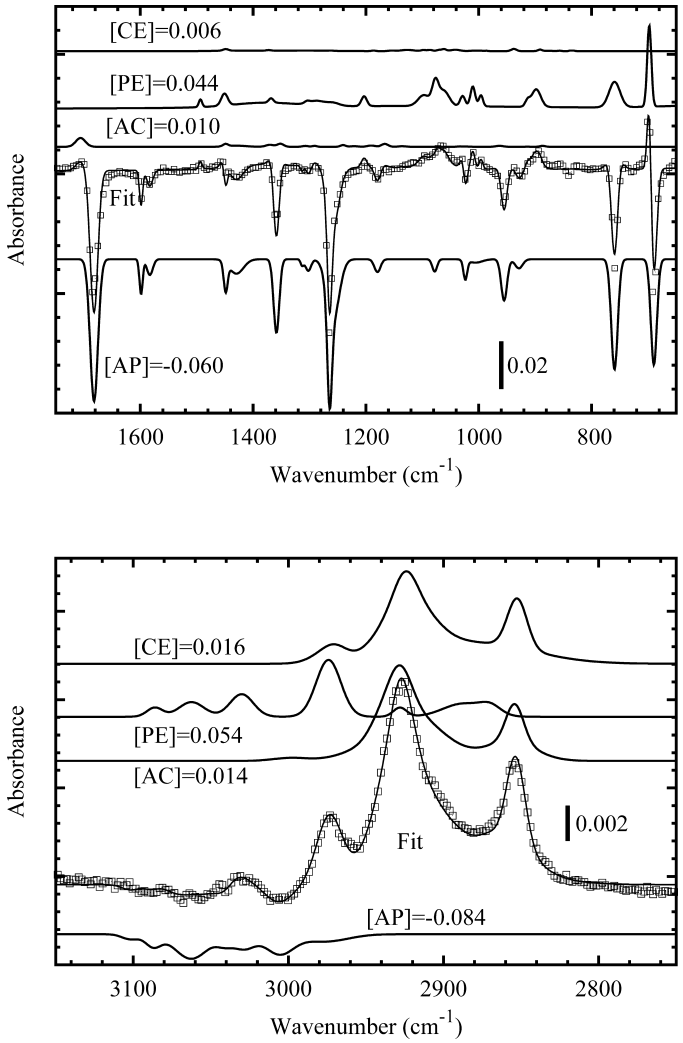

FIG. 3. Deconvolution of the evolution of the spectra during the sixth hour of the hydrogenation of AP in (**top**) the fingerprint and (**bottom**) the CH stretching range. Squares correspond to the experimental data while the line is the result of the fitting and the different components of the model.

we choose to work with the subtraction of two spectra measured during the reaction and not to perform any unsafe mathematical pretreatment. Examples of the deconvolution obtained with this method are presented in Fig. 3 for both FP and CH models corresponding to the variation of the solution during the sixth hour of AP hydrogenation at 80 °C. In these models, the number of variables is equal to the number of species, which makes the fitting effective and robust.

RESULTS AND DISCUSSION

Figure 3 shows typical results of the FP and CH model. Both fittings found a negative value for the reactant (AP) and a positive value for the products. Under the conditions of this study, AC, PE, and CE are the main products (concentration $>1\%$). The results discussed here are obtained with a model using four parameters: three individual concentrations (as we fixed the sum of the concentration to 0) and the last parameter corresponding to the baseline shift. For the FP model, the concentration of the reactant is calculated with a high accuracy, as in this range, its molar absorption is bigger than the bands due to the products. Numbers presented in Fig. 3 correspond to

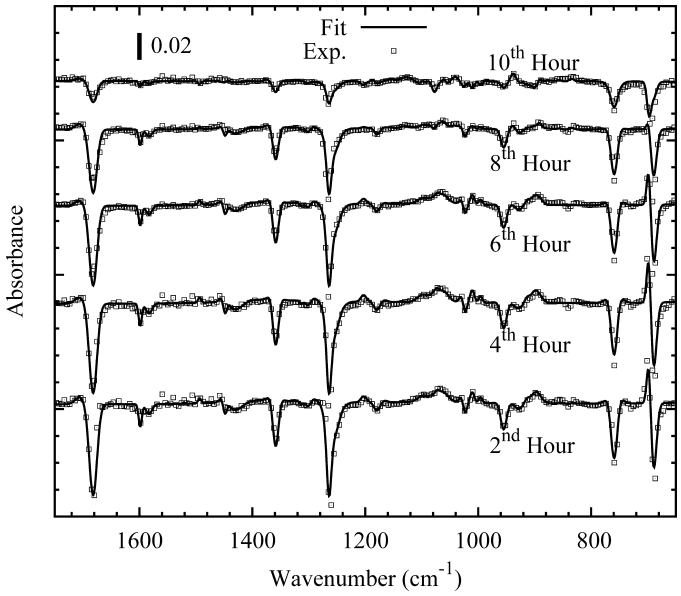

FIG. 4. Evolution of the spectra and their fitting during the hydrogenation in the fingerprint range.

the variation of concentration of different species calculated after fitting the models to the experimental spectra. The main product of the hydrogenation during the sixth hour is PE as all the most intense positive bands correspond precisely to that compound. A noticeable difference between the model and the experimental spectrum is situated at approximately 850 cm^{-1}. The model cannot simulate the negative band of the PF_6^- vibration as we chose not to involve the spectra of the IL suspension in the model. With the same apparatus, for the pure ionic liquid this specific band is saturated while all other bands are at least ten times smaller. Consequently, none of the other bands of the ionic liquid would be visible in the spectra and therefore perturb the modeling.

Figure 3 demonstrates the contrast between the two wavenumber ranges, as in the FP model most of the intense bands are negative, while in the CH model most of the bands are positive. Despite the obvious differences, after decomposition both models provide a similar picture with a loss of the reactant AP, with PE appearing as the main product. As the intensity of the molar absorptivity of AP in the CH range is relatively small compared to other species, this first model will not necessarily be very accurate in estimating the yield of the reaction. On the other hand, in the CH model, the molar absorptivities of the AC and CE bands (due to the cyclohexyl group) are much stronger, and thus this model will be better to estimate the selectivity in the case where hydrogenation is mainly taking place on the carboxyl group. In the FP range, the molar absorptivity of the reactant and possible products are comparable, and therefore this second model is more suitable to estimate the yield of the hydrogenation, or generally for cases where the selectivity of the hydrogenation is poor. Consequently, the information extracted from both CH and FP models are complementary.

Apart from this, the same fitting procedure is applied to analyze the evolution of the concentration of the reactant and products with time during the hydrogenation. Some results of the fitting procedure using the FP model, compared with the experimental spectra at several points in time, are presented in

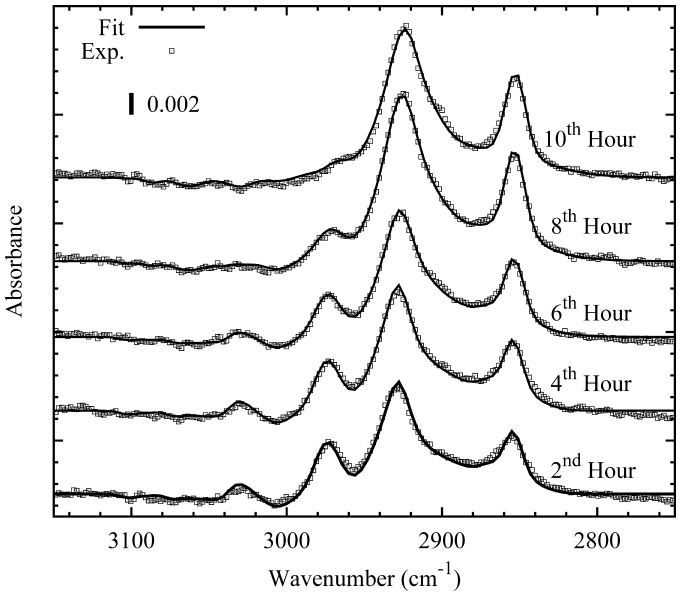

FIG. 5. Evolution of the spectra and their fitting during the hydrogenation in the CH stretching range.

Fig. 4. The FP model is complete enough to be able to fit the experimental data at various steps of the reaction. Some of the experimental spectra, in the range of 1500–1800 cm^{-1}, are not completely well represented by the model. This difference is due to the variation of water vapor in the spectrometer itself. Signals due to water vapor can be easily subtracted, but in this specific case, the concentration calculated with the model does not change noticeably after the subtraction of the water vapor spectrum. The two strong bands below 800 cm^{-1}, corresponding to out-of-plane CH bending modes,[41] do not look completely well simulated by this simple deconvolution. This problem appears to arise from the shift of the band with the change of environment during the hydrogenation process. The rest of the experimental spectra are well described by the FP model. The negative bands are decreasing after 6 hours, which probably corresponds to a decrease in the rate of the hydrogenation. Over the change of intensity, the shape of the spectra also clearly changes, which is an indication of the variation of the ratio between the different reactions with time. These variations will be described and quantified later in this discussion. While Fig. 4 illustrates the results of the FP model, the results of the fitting of the CH model on the experimental spectra are given in Fig. 5. The simple model using only four variables is also sufficient to follow the hydrogenation of AP. In this range, the intensity of the spectra does not decrease with time as with the FP model. The intensity of the two bands at 2925 and 2855 cm^{-1}, corresponding to the formation of the cyclohexyl group, are still fairly intense even after 10 hours, but on the other hand, the band at 2975 cm^{-1}, related to the species containing the hydroxyl group, almost disappears.

To describe in more detail the variation of the concentration of the four main substances during the first 12 hours of hydrogenation at room temperature (RT) and 80 °C, the results obtained with both models are depicted in Fig. 6. At RT, the yield of the hydrogenation of AP is decreasing slowly and linearly with time. The FP model states an estimation of around 2% of the initial concentration hydrogenated per hour. During the whole hydrogenation process the main products are first

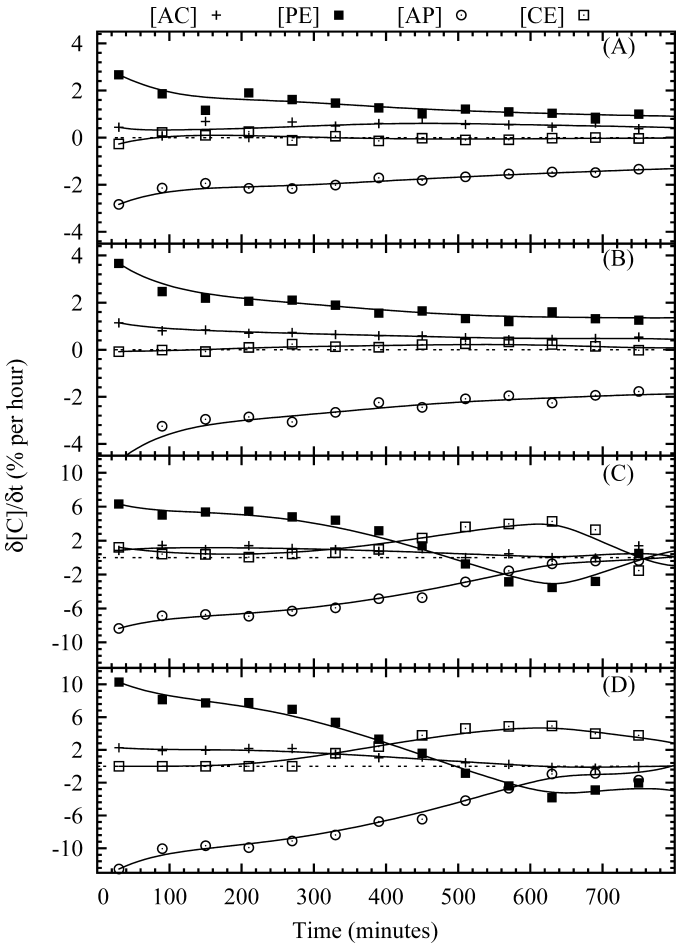

FIG. 6. Variation of the concentration of the reactant (AP) and products (PE, AC, CE) during hydrogenation. (**A**) and (**B**) correspond to the evolution at room temperature, calculated using the fingerprint and the CH stretching region, respectively. (**C**) and (**D**) correspond to the evolution at 80 °C calculated using the fingerprint and the CH stretching region, respectively.

PE, then AC, and finally CE. In contrast to the experiment at RT, during the hydrogenation at 80 °C the yield of the different products changes drastically with time. Initially, as at RT, the main product is PE, then AC, and finally CE, but, in both models, after 7 hours PE is no longer produced. The decrease of PE is coincident with the increase of the production of CE, which indicates that PE is hydrogenated to CE. Moreover, the velocity of the overall hydrogenation is also naturally faster at 80 °C than at RT, and both models give a yield three times greater at 80 °C than at RT.

Another way to describe the kinetics of the hydrogenation is to integrate the variation of the concentration calculated (shown in Fig. 6) and thereby obtain the evolution of the concentrations of the four species, which is presented in Fig. 7. Identical conclusions can be drawn with both multivariate models and from GC measurements: the reaction at RT was far from being complete, as after 12 hours the conversion was only 20% and the consumption of the reactant still proceeded linearly with time, as did the increase of the concentration of the products. The experiment at higher temperature also mainly yielded PE as product, but in this case its concentration reached a maximum after 7 hours. The PE selectivity of the hydrogenation calculated from both multivariate models has been calculated and regrouped in Fig. 8B, while the PE selectivity

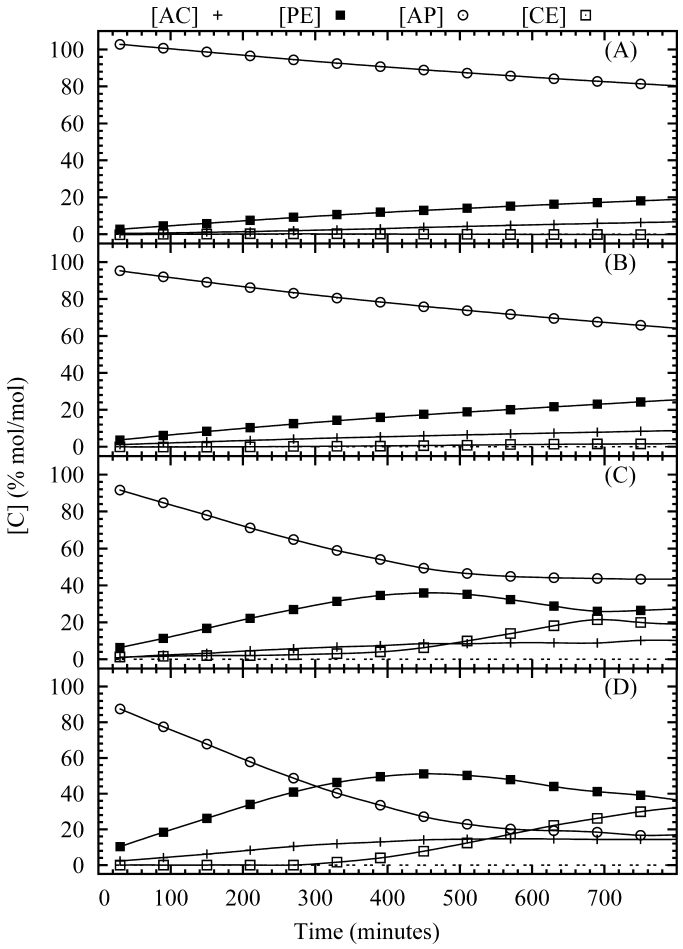

FIG. 7. Evolution of the concentration of the reactant (AP) and products (PE, AC, CE) during hydrogenation. (**A**) and (**B**) correspond to the evolution at room temperature, calculated using the fingerprint and the CH stretching region, respectively. (**C**) and (**D**) correspond to the evolution at 80 °C calculated using the fingerprint and the CH stretching region, respectively.

calculated from the variation of concentration within an hour is shown in Fig. 8A. At RT the selectivity decreases slowly with time, which can be attributed to the consecutive aromatic ring hydrogenation of PE. At higher temperature the selectivity drops rapidly after 7 hours. Figure 8B shows the evolution of the "instantaneous" PE selectivity; in that case the selectivity drops even faster and shows two different trends with a selectivity of around 80% during the first five hours, and then PE is predominantly hydrogenated and produces CE.

Selectivities calculated from both models were confirmed by the results obtained from GC measurements, which are generally more accurate. Both models, FP and CH, are therefore suitable to describe the concentration profiles of reactant/products during hydrogenation. The FP model appears more suitable to follow the consumption of the reactant (AP), while the CH model shows a better description of the product distribution due to higher weighting of bands in the CH region. This behavior indicates that the choice of the most suitable model will depend greatly on the vibrational bands that are dominant in the spectra of the reaction mixture. GC measurements performed at the end of the hydrogenation reaction indicated that the CH model provided a certain systematic underestimation of the conversion, probably due to the fact that the intensity of the products in the CH region is

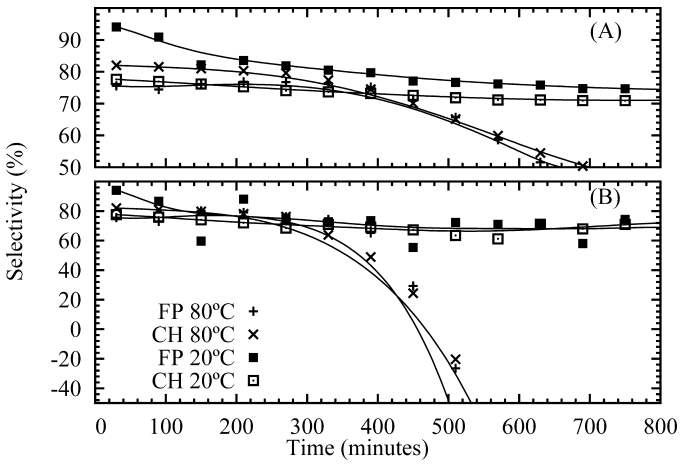

FIG. 8. (**A**) Selectivity and (**B**) "instantaneous" selectivity of the hydrogenation using the fingerprint and the CH stretching region at room temperature and 80 °C

rather low. However, this underestimation never exceeded 10%. Nevertheless, ATR measurements coupled with multivariate analysis offer striking advantages compared to GC sampling and should be considered to study reaction kinetics or to perform reaction parameter screenings, even with a reaction system containing competing and consecutive reactions, as this approach is *in situ*, efficient, and robust and does not require invasive sampling, which is a problem especially for high pressure reactions.

CONCLUSION

A simple model based on the deconvolution of a spectrum by the individual spectra of the main components of the reaction mixture was developed and applied to a catalytic chemo-selective hydrogenation. The first step of the analysis consisted of creating a simple function representative of the main information included in each reactant or product spectrum. Then, the spectrum of the solution was deconvoluted using these representative functions. The results obtained by both models, focusing either on FP or CH regions, gave an *in situ* qualitative analysis of the composition of the solution. The evaluation of FP and CH models for the description of the changes in the product distribution during hydrogenation of AP showed that the choice of a suitable model greatly depends on the vibrational bands that are most prominent in the spectra of the reaction mixture. Due to different molar absorptivity of the reactant and products, the CH model is considered the superior model regarding the quantitative analysis of the selectivity, specifically when PE is the main product of the reaction. The main limitations of the system arise from the sensitivity of some bands to their environment. The OH and C=O stretching bands must be dealt with very carefully in this type of analysis.

The combination of *in situ* ATR and multivariate analysis proved to be a powerful approach for investigating the changes of the concentrations of the various products formed during the high pressure heterogeneous catalytic gas–liquid phase reaction. In the case of a simple reaction, the analysis of the evolution of the intensity of a unique band can be sufficient to follow the reaction progress. In a more complex system, such as the one analyzed in this study, with competitive reactions and strong overlapping of the bands of different components,

this type of univariate analysis is impossible. In this case, the deconvolution of the spectrum by the spectra of the main components offers the opportunity to follow the progress of the reaction and distribution of the products without disturbing the reaction by taking samples for outside analysis.

ACKNOWLEDGMENT

We thank the Bundesamt für Energie (BFE) for financial support of this work.

1. G. Mul, G. M. Hamminga, and J. A. Moulijn, Appl. Spectrosc. **34,** 109 (2004).
2. T. Bürgi and A. Baiker, Adv. Catal. **50,** 227 (2006)
3. A. R. Almeida, J. A. Moulijn, and G. Mul, J. Phys. Chem. C **112,** 1552 (2008).
4. G. M. Hamminga, G. Mul, and J. A. Moulijn, Chem. Eng. Sci. **59,** 5479 (2004).
5. J. D. Grunwaldt and A. Baiker, Phys. Chem. Chem. Phys. **7,** 3526 (2005).
6. G. M. Hamminga, G. Mul, and J. A. Moulijn, Appl. Spectrosc. **61,** 470 (2007).
7. F. Gao, R. Li, and M. Garland, J. Mol. Catal. A: Chem. **272,** 241 (2007).
8. C. W. Scheeren, J. B. Domingos, G. Machado, and J. Dupont, J. Phys. Chem. C **112,** 16463 (2008).
9. M. Burgener, R. Furrer, T. Mallat, and A. Baiker, Appl. Catal., A **268,** 1 (2004).
10. N. M. Bertero, C. R. Apesteguía, and A. J. Marchi, Appl. Catal., A **349,** 100 (2008).
11. C. P. Casey, S. E. Beetner, and J. B. Johnson, J. Am. Chem. Soc. **130,** 2285 (2008).
12. D. G. Blackmond, M. Ropic, and M. Stefinovic, Org. Process Res. Dev. **10,** 457 (2006).
13. F. Gao, A. D. Allian, H. Zhang, S. Cheng, and M. Garland, J. Catal. **241,** 189 (2006).
14. M. S. Schneider, J.-D. Grunwaldt, T. Burgi, and A. Baiker, Rev. Sci. Instrum. **74,** 4121 (2003).
15. S. D. Lin, D. K. Sanders, and M. Albert Vannice, Appl. Catal., A **113,** 59 (1994).
16. F. Alonso, P. Riente, F. Rodríguez-Reinoso, J. Ruiz-Martínez, A. Sepúlveda-Escribano, and M. Yus, J. Catal. **260,** 113 (2008).
17. A. Drelinkiewicza, A. Waksmundzka, W. Makowski, J. W. Sobczak, A. Krol, and A. Zieba, Catal. Lett. **94,** 143 (2004).
18. C.-S. Chen, H.-W. Chen, and W.-H. Cheng, Appl. Catal., A **248,** 117 (2003).
19. L. P. Christensen, M. Edelenbos, and S. Kreutzmann, "Fruits and Vegetables of Moderate Climate", in *Flavours and Fragrances - Chemistry, Bioprocessing and Sustainability*, R. G. Berger, Ed. (Springer, New York, 2007).
20. R. Sheldon, Chem. Commun. **23,** 2399 (2001).
21. J. W. Hutchings, K. L. Fuller, M. P. Heitz, and M. M. Hoffmann, Green Chem. **7,** 475 (2005).
22. M. J. Earle, J. Esperanca, M. A. Gilea, J. N. C. Lopes, L. P. N. Rebelo, J. W. Magee, K. R. Seddon, and J. A. Widegren, Nature (London) **439,** 831 (2006).
23. C. W. Scheeren, G. Machado, S. R. Teixeira, J. Morais, J. B. Domingos, and J. Dupont, J. Phys. Chem. B **110,** 13011 (2006).
24. P. Migowski and J. Dupont, Chem. Eur. J. **13,** 32 (2007).
25. Y. Gu and G. Li, Adv. Synth. Catal. **351,** 817 (2009).
26. J. Dupont, G. S. Fonseca, A. P. Umpierre, P. F. P. Fichtner, and S. R. Teixeira, J. Am. Chem. Soc. **124,** 4228 (2002).
27. S. G. Kazarian, M. F. Vincent, F. V. Bright, C. L. Liotta, and C. A. Eckert, J. Am. Chem. Soc. **118,** 1729 (1996).
28. J.-M. Andanson, F. Jutz, and A. Baiker, J. Phys. Chem. B **113,** 10249 (2009).
29. R. G. Brereton, Analyst (Cambridge, U.K.) **125,** 2125 (2000).
30. G. M. Escandar, A. C. Olivieri, N. M. Faber, and H. C. Goicoechea, A. Muñoz de la Peña, and R. J. Poppi, Trends Anal. Chem. **26,** 752 (2007).
31. K. L. A. Chan, N. Elkhider, and S. G. Kazarian, Chem. Eng. Res. Des. **83,** 1303 (2005).
32. E. Kriesten, F. Alsmeyer, A. Bardow, and W. Marquardt, Chemom. Intell. Lab. Syst. **91,** 181 (2008).
33. T. R. Jensen, R. P. Van Duyne, S. A. Johnson, and V. A. Maroni, Appl. Spectrosc. **54,** 371 (2000).
34. F. Jutz, J.-M. Andanson, and A. Baiker, J. Catal. **268,** 356 (2009).
35. E. Widjaja, C. Z. Li, W. Chew, and M. Garland, Anal. Chem. **75,** 4499 (2003).
36. P. Lalanne, J. M. Andanson, J. C. Soetens, T. Tassaing, Y. Danten, and M. Besnard, J. Phys. Chem. A **108,** 3902 (2004).
37. J. M. Andanson, J. C. Soetens, T. Tassaing, and M. Besnard, J. Chem. Phys. **122,** 174512 (2005).
38. M. C. R. Symons and G. Eaton, J. Chem. Soc. Faraday Trans. I **81,** 1963 (1985).
39. R. Thijs and T. Zeegershuyskens, Spectrochim. Acta, Part A **40,** 307 (1984).
40. M. Savolainen, A. Heinz, C. Strachan, K. C. Gordon, J. Yliruusi, T. Rades, and N. Sandler, Eur. J. Pharm. Sci. **30,** 113 (2007).
41. A. Gambi, S. Giorgianni, A. Passerini, R. Visinoni, and S. Ghersetti, Spectrochim. Acta, Part A **36,** 871 (1980).